Oxidized Titanium Screws Coated with Calcium Ions and Their Performance in Rabbit Bone

Young-Taeg Sul, DDS, PhD[1]/Carina B. Johansson, PhD[2]/Tomas Albrektsson, MD, PhD, ODhc[3]

Purpose: *The aim was to answer a fundamental question: Do the chemical properties of titanium implants influence osseointegration?* ***Materials and Methods:*** *Screw-type implants produced of turned commercially pure (grade 1) titanium (controls) and electrochemically calcium-deposited titanium implants (Ca test implants) were placed in the tibiae and femora of a total of 10 mature New Zealand white rabbits. The macro arc oxidation method was applied for Ca implants. Surface oxides were characterized with different analytic techniques, including x-ray photoelectron spectroscopy, auger electron spectroscopy, scanning electron microscopy, thin-film x-ray diffractometry, and TopScan 3D. The bone response was evaluated by biomechanical tests, histology, and histomorphometry.* ***Results:*** *After a follow-up period of 6 weeks, test Ca implants showed a significant increase in mean peak removal torque (P = .0001) and in the histomorphometric measurement of bone-to-metal contact around the implants (P = .028) in comparison to controls. In addition, more mature mineralized bone was observed adjacent to test Ca implants compared to controls, as evaluated on 10-μm undecalcified, toluidine blue–stained, cut, and ground sections.* ***Discussion:*** *The potential role of surface Ca chemistry to a superior bone response is discussed with specific reference to interaction with Ca^{+}-binding proteins and function as binding sites of calcium phosphate mineral.* ***Conclusion:*** *The present results suggest that the surface chemical composition of titanium implants is of great importance for the bone response. Ca ion–deposited titanium implants showed fast and strong osseointegration in the rabbit bone model.* (Int J Oral Maxillofac Implants 2002;17:625–634)

Key words: *bone response, histomorphometry, osseointegration, removal torque, titanium oxides*

Numerous surface modifications of endosseous implants have been carried out to allegedly improve surface quality, resulting in the enhancement of clinical outcomes of oral implants.[1–4] It is generally known that the bone response to implant surfaces is related to many different surface properties, most likely involving topographic/morphologic properties of the implant surface.[5–8] The chemical properties of the implant surface are also important.[9–12] Surface chemistry of endosseous implants has been influenced by a great number of technologies, such as simple soaking/immersion treatment,[13,14] various calcium (Ca) phosphate coating methods,[15,16] sol gel–derived coatings,[17,18] electrochemical oxidation,[19,20] chemical vapor deposition,[21] physical vapor deposition,[22] ion beam–assisted/enhanced deposition,[23,24] and plasma immersion ion/ion implantation with differently applied ions.[25] Many of those investigations have focused extensively on so-called "bioactivity"—metal coatings of potentially bioactive materials such as various types of hydroxyapatite (HA) or other Ca phosphate compounds, bioglass, and bioceramics.[26–28] However, bioactive implants have revealed drawbacks, such as insufficient mechanical properties (intra- and/or

[1]Researcher, Department of Biomaterials/Handicap Research, Institute for Surgical Sciences, University of Göteborg, Sweden; Osseointegration Research Institute, Seoul, Korea.
[2]Associate Professor, Department of Biomaterials/Handicap Research, Institute for Surgical Sciences, University of Göteborg, Sweden.
[3]Professor, Chairman, and Head, Department of Biomaterials/Handicap Research, Institute for Surgical Sciences, University of Göteborg, Sweden.

Reprint requests: Dr Young-Taeg Sul, Department of Biomaterials/Handicap Research, Institute for Surgical Sciences, Göteborg University, Box 412, SE-405 30 Göteborg, Sweden. Fax: +46 31 773 2941. E-mail: young-taeg.sul@hkf.gu.se

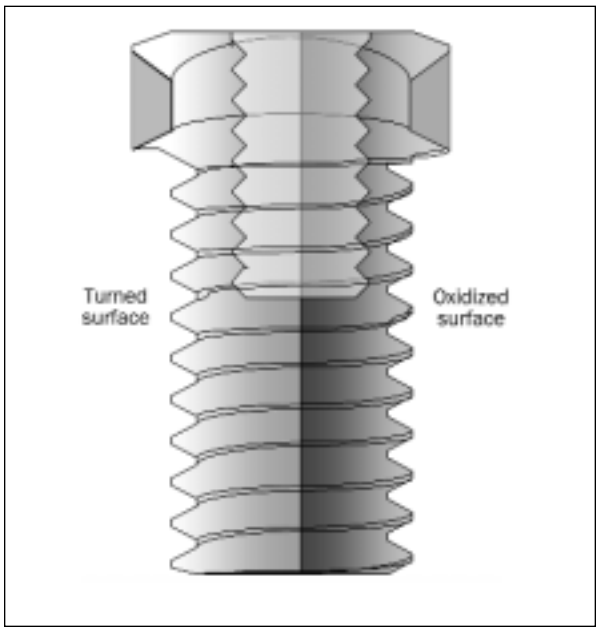

Fig 1 The implant was designed with a tetragonal head and an inner threaded part allowing biomechanical tests. The samples used for histomorphometry had 2 surfaces: one half *(left)* is a turned native oxide surface, and the other half *(right)* is the test Ca surface.

interfacial failure of coating materials) and biodegradation/bioresorption during biologic function.[29–31] To cite one example, HA-coated implants have not been documented to date with positive 5-year clinical results, despite being used for more than 15 years.[32]

In the present study, an electrochemically Ca ion–deposited oxidized titanium implant was evaluated, which has substantially different chemical composition compared to HA, other Ca phosphates, or other bioactive materials that typically contain SiO_2, CaO, and P_2O_5 plus additional oxides. The main aim of the present study was to investigate the bone tissue response to the electrochemically Ca ion–deposited oxidized implant in a rabbit bone model.

For further understanding of the relationship between bone tissue reactions and surface oxide properties of the titanium implant, the latter were characterized by various surface analytic techniques, including auger electron spectroscopy (AES), scanning electron microscopy (SEM), thin-film x-ray diffractometry (TF-XRD), x-ray photoelectron spectroscopy (XPS), and confocal laser scanning profilometry (TopScan 3D) (Heidelberg Instruments, Heidelberg, Germany). Bone tissue reactions were evaluated by biomechanical testing, histology, and histomorphometry after a follow-up period of 6 weeks in rabbit bone.

The surface Ca chemistry has been provided by different techniques, preferably Ca ion implantation.[9,33–36] The authors' group has been carrying out investigations on bone tissue response to a series of surface chemistry modifications using electrochemical oxidation. The animals of the present study have been used in separate investigations of a series of oxidized implants. All data with respect to Ca-reinforced titanium implants is published in this paper, and the other parts of findings are published separately.[37,38]

MATERIALS AND METHODS

Implant Design and Preparation

Screw-type implants with a pitch height of 0.5 mm, outer diameter of 3 mm, length of 7.2 mm, a 3.2-mm square head, and an inner threaded hole of 2 mm, were turned from 5-mm rods of commercially pure titanium (ASTM Grade 1). In the present study, 2 groups of titanium screws were used: as-turned implants were used as the control group, and the other electrochemically oxidized implants comprised the test Ca group. The test Ca implants were prepared using micro arc oxidation (MAO) at high anodic forming voltages and current densities at galvanostatic mode in a Ca-containing mixed electrolyte system. During MAO, the anodic forming voltage with slope dV/dt was controlled at ≤ 0.5 with combined electrochemical parameters. A comprehensive description of the electrochemical oxidation method may be found in a previous study.[20]

For the histomorphometric evaluation, "double-faced" surfaces on each implant were designed (Fig 1); one half of the implant had a surface of the test Ca implant, and the other half had the control surface of the turned implant. This implant design allowed direct comparison between control and test surfaces in the same biologic sites. Implants for biomechanical tests were either turned or test Ca surfaces.

Chemical Composition and Surface Characteristics of Implants

All surfaces of control and Ca implants consisted mainly of titanium dioxide (TiO_2). Carbon was detected as a surface contaminant. Some traces, such as sodium, calcium, silicon, etc, were present but disappeared to noise level after argon ion sputter cleaning of some 1.4 nm thickness. Test Ca implants contained Ca cations electrochemically incorporated into the TiO_2 matrix from a Ca-containing mixed electrolyte system during the MAO process. XPS survey spectrum of the Ca implant detected the presence of the Ca elements (Fig 2). High-resolution XPS spectrum revealed that doublet peak line

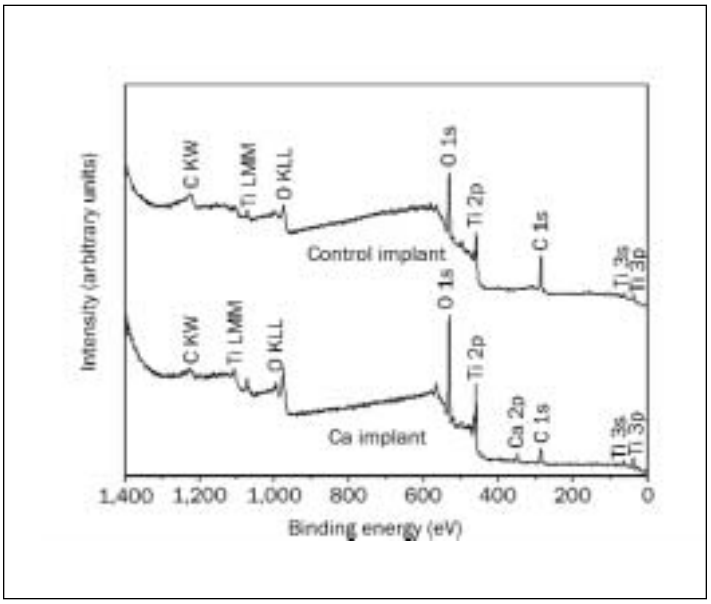

Fig 2 XPS survey spectra of a turned screw (control) implant and an electrochemically oxidized screw (test) Ca implant at the binding energy up to 1,400 eV. There are almost the same peak positions between the 2 group samples, except Ca 2p peaks for test Ca implants.

position of Ca $2p_{1/2}$ was detected at about 351.4 eV and $2p_{3/2}$ at about 347.8 eV (Δ = 3.6 eV) (Figs 3a and 3b). These peak positions indicate that Ca may exist in the Ca titanates, such as $CaTiO_3$, at the outermost surface. Furthermore, depth profiles by AES measurement of the Ca implant showed that the Ca element is incorporated throughout the titanium oxide during the MAO process (Figs 4a and 4b).

Relative atomic concentrations at the outermost surface were approximately Ca ≤ 11%. The oxide thickness was evaluated as 17 ± 6 nm for controls and 1,296 ± 225 nm for Ca implants as measured at 3 different locations on the implant (1 thread top, 1 thread valley, and in the bottom of the implant). SEM showed a nonporous structure in controls and a porous structure in the Ca implants (Figs 5a and 5b). The pore size of Ca implants was ≥ 1.3 μm in diameter. TF-XRD patterns showed amorphous for controls and anatase phase for Ca samples (Figs 6a and 6b). The surface roughness parameter Sa (height deviation from the mean plane) was in the range of 0.83 ± 0.32 μm for control implants and 0.85 ± 0.32 μm for the test implants as measured with a confocal laser scanning profilometer (TopScan 3D). The corresponding roughness parameter Scx (average distance between the surface irregularities in spatial direction) was 9.78 ± 1.40 μm for control implants and 9.83 ± 1.07 μm for test implants. The surface oxide characteristics of titanium implants used in this study are summarized in Table 1. Further details of surface analyses are described in a previous study.[39]

Animals and Surgical Technique

A total of 10 mature (mean weight of 2.5 kg) New Zealand white rabbits of both sexes were used in this study, which was approved by the local animal ethics committee at the University of Göteborg, Sweden. Each rabbit received a total of 8 implants: 3 implants were placed adjacent to the tibial tuberosity penetrating 1 cortical layer only in each leg, and 1 implant ("double-faced surfaces") was placed in each distal femoral region. For surgery, the animals were anesthetized with intramuscular injections of fentanyl and fluanison (Hypnorm Vet, Janssen, Saunderton, England) at a dose of 0.5 mL/kg body weight and intraperitoneal injections of diazepam (Kabi Pharmacia, Helsingborg, Sweden) at a dose of 2.5 mg per animal. The skin and fascial layers were opened and closed separately. The periosteal layer was gently pulled away from the surgical area and was not resutured. During all surgical drilling sequences, low rotary drill speeds (not exceeding 2,000 rpm) and saline cooling were used. The animals were kept in separate cages, and immediately after surgery they were allowed to bear their full weight on their legs. After a follow-up period of 6 weeks, the animals were sacrificed by intravenous injections of Pentobarbitalum (Apoteksbolaget, Uppsala, Sweden) as prescheduled.

Specimen Preparation and Analysis

The 3 implants in each tibia were selected for removal torque tests, while the 1 implant ("double-faced" surface) in each femur was processed for later

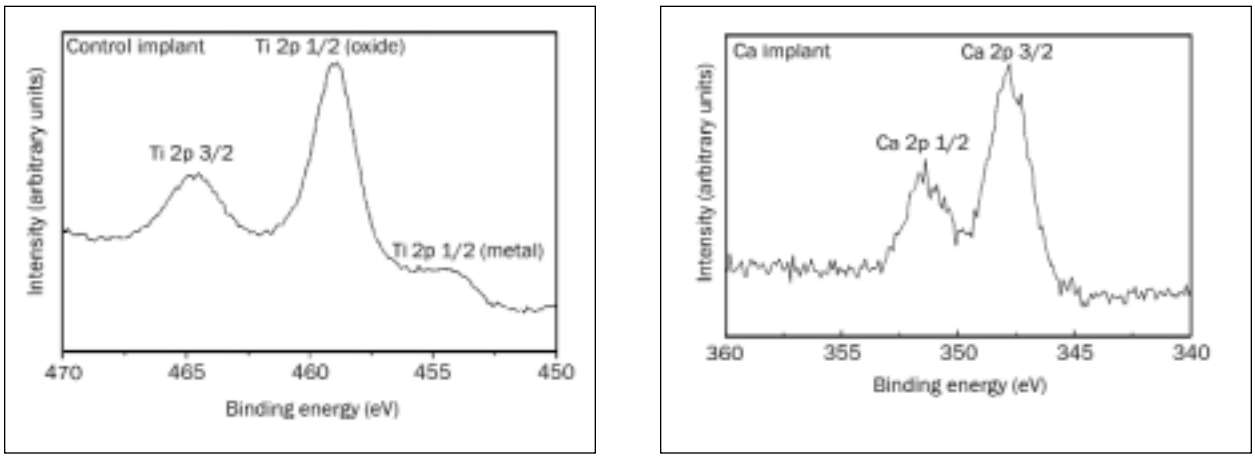

Figs 3a and 3b High-resolution XPS spectrum of Ti 2p for the control and Ca 2p for the Ca implant. The Ca 2p shows doublet peak line positions at about 351.4 eV and 347.8 eV. This indicates that Ca may be present in an oxidized form.

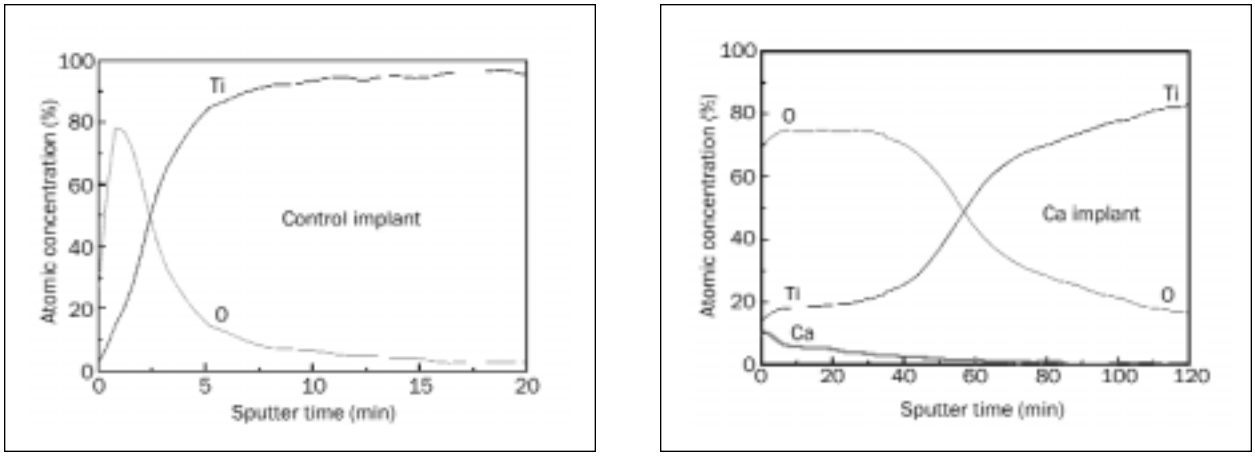

Figs 4a and 4b AES concentration depth profiles from the control and test Ca screw implants. The Ti, O, and Ca profiles are presented. Ca is distributed throughout the oxide and decreases from approximately relative atomic concentrations 11 at % (E_p = 4.0 keV, I_p= 300 nA).

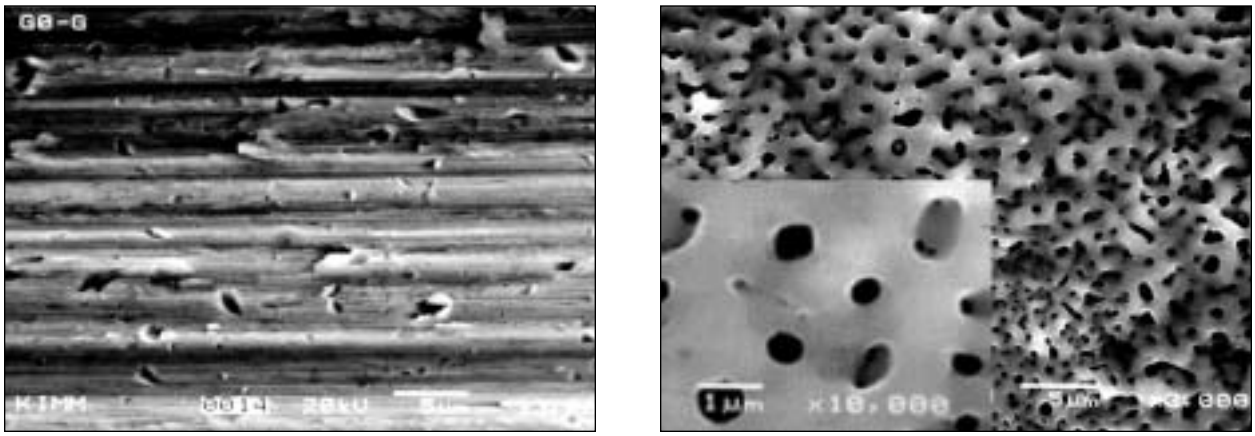

Figs 5a and 5b SEM photographs show a nonporous microstructure of the turned (control) implant and a porous microstructure of the test Ca implant. The pore size on the test Ca implant is ≤ 1.5 μm in diameter (original magnification ×3,000; ×10,000 inset).

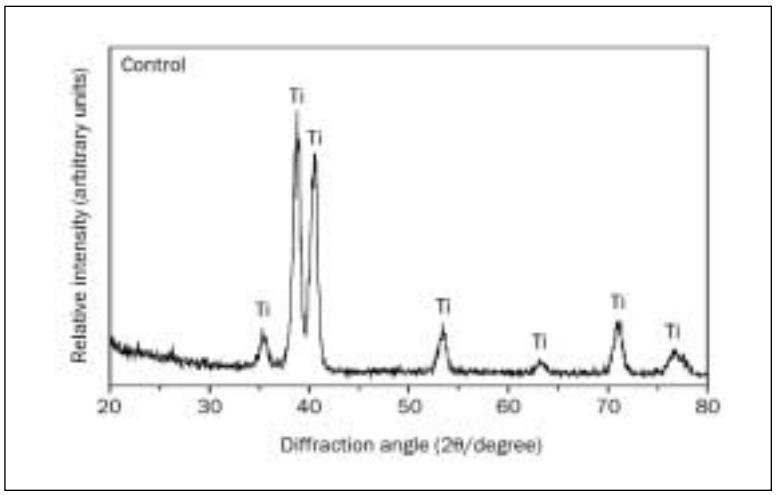

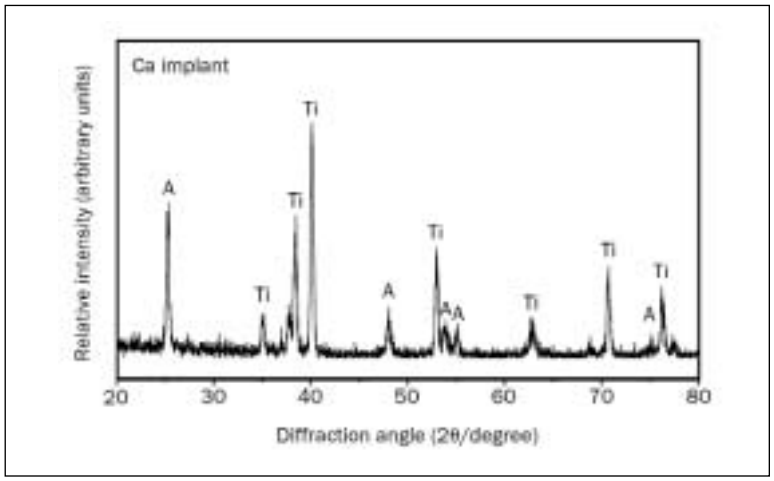

Figs 6a and 6b XRD spectra measured on the plate sample abraded by # 800 silicon carbide paper control and the plate electrochemically oxidized in the same way as was done for the test Ca implant. XRD patterns show amorphous titanium oxide for the control and an anatase type of crystal structure for the test Ca implant. Ti = titanium; A = anatase.

Table 1 Surface Oxide Characteristics of the Control and Electrochemically Treated Groups

Oxide characteristics	Control implant	Ca implant
Chemical composition[1]	Primarily TiO_2 and C	Primarily TiO_2 and Ca, traces of C, P, Na, Si
Oxide thickness[2]	17 ± 6 nm	1296 ± 225 nm
Morphology[3]	Nonporous structure with turned grooves ≤ 10 μm	Porous structure with a number of craters
Pore size distribution[3]	N/A	≤ 1/3 μm by length
Crystallinity[4]	Amorphous titanium oxide	Anatase titanium oxide
Roughness (Sa)[5]	0.83 ± 0.32 μm	0.85 ± 0.32 μm
Roughness (Scx)	9.78 ± 1.40 μm	9.83 ± 1.07 μm

[1]As determined by XPS with both monochromatic and achromatic x-ray sources.
[2]As measured by continuous sputter etching with 4K eV Ar ion in AES at 4 different locations of each implant: 1 thread top, one thread valley, and in the head of the screw implant.
[3]Characterized by SEM.
[4]As measured by TF-XRD on the plate sample treated under the same experimental conditions as the screw-shaped implant.
[5]As measured with confocal laser scanning profilometer (TopScan 3D) with 245 μm × 245 μm of measuring area, on the 3 thread tops, 3 thread valleys, and 3 thread flanks each making 27 measurements for each group. Sa presents the height deviation from the mean plane. Scx presents the average distance between the surface irregularities in spatial direction.

histologic and histomorphometric evaluations on cut and ground sections. The number of control and Ca implants used in the present study was as follows: controls—15 implants used for removal torque tests, 7 implant surfaces for histomorphometric quantifications; Ca implants—17 implants for removal torque tests, 7 surfaces for histomorphometry. The surface of the control implants consisted mainly of TiO_2. The surface of the Ca test implants consisted mainly of TiO_2 plus electrochemically incorporated Ca cations.

Removal Torque Tests. Removal torque is a 3-dimensional test reflecting an implant's interfacial shear strength; it is routinely used and well documented.[5,40] The equipment consists of an electronic device incorporating a strain-gauged transducer, enabling controlled torque analysis of the peak loosening torque. The device ensures a fixed rotation rate in contrast to hand-controlled devices to eliminate the "operator errors," and it has been shown to achieve high reproducibility and low operator sensitivity. Immediate quantitative in vivo results of the implant loosening torque, in Ncm, are obtained with this test. Measurements of peak removal torque were performed on the implants placed in each tibia after 6 weeks of healing.

Histomorphometric Evaluations. At the sacrifice of the rabbits 6 weeks after surgery, the implants were removed en bloc and immersed in fixative, allowing subsequent routine histologic and histomorphometric investigations. Undecalcified cut and ground sections were prepared with the Exakt system (Exakt Apparatebau, Norderstedt, Germany).[41] One central section was taken from each sample. The sections were then ground to a final thickness of about 10 µm prior to staining. Sections for histomorphometry were stained in 1% toluidine blue in 1% borax solution, mixed in a 4:1 proportion with 1% pyronin-G solution prior to qualitative and quantitative observations in the light microscope. Computer-based histomorphometric analyses of the stained toluidine blue sections were performed in a Leitz Aristoplan light microscope equipped with a Leitz Microvid unit (Wetzlar, Germany), connected to a personal computer and mouse. This enabled the observer to perform quantifications directly in the eyepiece of the microscope, with oculars of 10× and a zoom of 2.5×. Histomorphometric investigations involved quantification of the bone-to-metal contact (BMC). In addition, qualitative observations of the tissue structures around the implants were also performed in the light microscope.

Statistics

Statistical analyses of the removal torque measurements were performed using the Mann-Whitney *U* test. The histomorphometric measurements were analyzed using the Wilcoxon signed rank test, since test and control group implants were paired (see "double-faced" surfaces in Fig 1). Differences were considered statistically significant at $P < .05$ and highly significant at $P < .01$.

RESULTS

Removal Torque Measurement

Ca implants revealed a highly significant increase in the mean peak value of removal torque when compared to control (turned) implants. The mean peak values of removal torque were 12.7 ± 1.8 Ncm (range 10 to 15 Ncm) for control implants and 19.4 ± 3.1 Ncm (range 14 to 24 Ncm) for test Ca implants ($P = .0001$). The difference in removal torque was 53%. Figure 7 demonstrates the differences in mean peak value of removal torque obtained from control (turned) implants and test Ca implants after 6 weeks of implant placement.

Histomorphometric Evaluations

The mean BMC value in all implant threads of the Ca implants demonstrated a significant increase of 272% compared to paired control implants. The mean BMC was 18 ± 8% (range 6% to 30%) in paired control implants and 49 ± 12% (range 31% to 64%) in test Ca implants ($P = .028$). Figure 8 shows comparisons of the BMC in all threads between paired control implants and test Ca implants after 6 weeks of implant placement.

Qualitative Observations

There were distinct differences between mineralization and apposition of new bone formed at the bone-implant interface between test and control implants. Ca implants demonstrated more homogeneously mineralized bone in close contact with the implant surface (Fig 9a), while control surfaces were interfaced with an osteoid layer that was less mineralized (Fig 9b). In addition, the newly formed bone at the implant interface was found spread more diffusely along the implant surface, in comparison with the situation at the control implants (Figs 9a and 9b). Inflammatory cells such as macrophages and multinuclear giant cells were detected on both test and control surfaces.

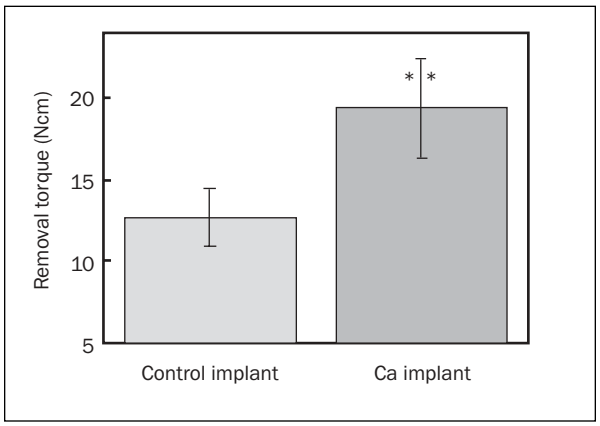

Fig 7 The test implant demonstrated a highly significant increase in mean removal torque values (Ncm) after a follow-up of 6 weeks compared to the control implant (***P* = .0001).

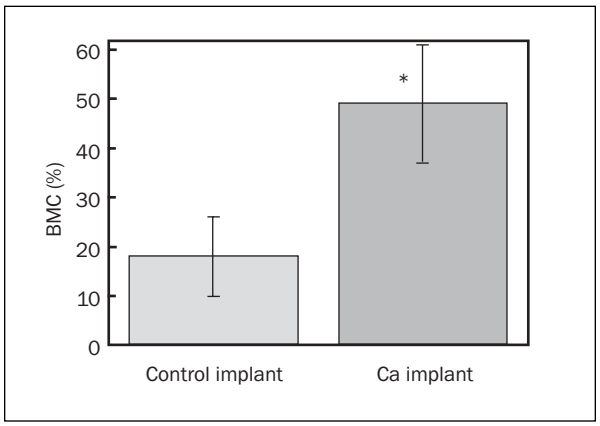

Fig 8 The test implant demonstrated a significant increase in the mean BMC (bone-to-metal contact) after a follow-up of 6 weeks compared to the control implant (**P* = .028).

Fig 9a Test Ca implant: Undecalcified cut and ground section of a test sample demonstrates its osteoconductive surface, ie, a higher degree of "direct contact" between mostly bone tissue and the Ca implant surface, as compared to the control surface. Osteocytes were observed in close relation to the test Ca implant surface. Ongoing bone formation is clearly visible with osteoid rim as covered with osteoblasts *(arrows).* Bar = 100 µm.

Fig 9b Control implant: Undecalcified cut and ground section of a control sample demonstrates less bony contact, with soft tissue areas *(asterisks)* in close relation to the implant surface. Bar = 100 µm.

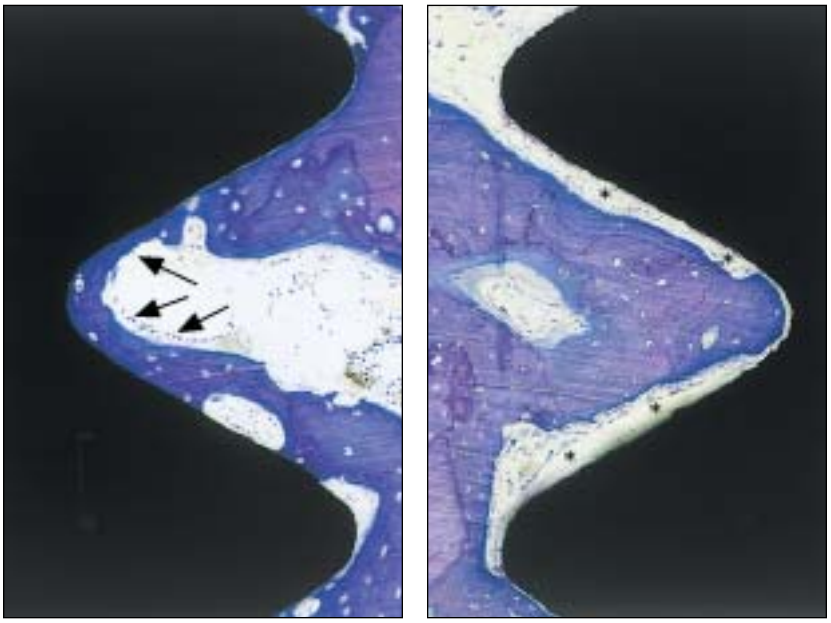

DISCUSSION

The MAO process used in the present study has been demonstrated to be capable of producing surface chemistry modifications, as well as changing morphologic and physical properties of screw-type titanium implants. Alterations of the chemical composition include electrochemical deposition of Ca cations, shown in the present study, and also S and P anions, respectively, in the titanium oxide matrix, as described in a previous study.[38] The altered morphologic and physical properties have likewise been described in previously published papers.[8,39] The observed pore/crater of the microporous surface structure is of potential interest since it may allow carriers of growth factors or bone morphogenetic proteins. The pore configurations, such as pore size and porosity, can be controlled in a certain range by electrochemical parameters such as the oxide-forming voltage, the current density, and the electrolyte composition.[20,39]

What oxide properties of the titanium implants are then responsible for the significantly improved bone responses in the present study? One possible explanation relates to morphologic and physical changes of surface oxide properties, characterized by titanium oxide that is 1,290 nm thicker and anatase type of oxide crystallinity, as suggested by Sul and coworkers.[8,42,43] In general, the osseointegration of machined, turned implants and recently developed novel types of rougher surface implants has been explained by the ingrowth of bone into

micro- and macroscopic surface irregularities.[5,6,44] However, since the roughness (Sa and Scx) of test Ca implants and controls was nearly the same, despite differences of the surface structures in the present study, differences in surface roughness cannot explain the present results. Differing chemical properties of test Ca implants and controls (Table 1), ie, the surface Ca chemistry of Ca implants, may be the best possible explanation for the reinforced osseointegration. With respect to the surface chemical properties, it should be noted that the Ca implants in the present study showed substantial differences of their chemical compositions from so-called "bioactive implants" coated with bioactive materials (most commonly SiO_2, CaO, and P_2O_5 together plus additional oxides) and Ca phosphate compound–based implants.

In the literature, there is a dearth of information on in vivo bone responses to Ca surface chemistry of titanium implants. Hanawa and associates[9] and Takamura and colleagues[45] investigated Ca ion–implanted titanium surfaces in rabbit bone and observed histologically more new bone formed on the Ca^{2+} side than on the titanium side at 2 and 8 days after surgery. They also reported that neither macrophage nor inflammatory cell infiltration was observed at 2 and 8 days, respectively. However, Howlett[46] questioned whether any new bone was formed within 2 days. Present histologic findings clearly showed macrophages and multinuclear giant cells on 10-μm undecalcified, cut, and ground sections stained with toluidine blue. This disagreement may be the result of the staining methods, as well as section thicknesses (50 μm in their sections). Ichikawa and coworkers[34] reported that the bone volume of Ca ion–mixing titanium was larger than that of HA.

How surface chemistry of Ca implants (Ca ≤ 11% incorporation into TiO_2 matrix) in the present study affects the strong bone response is not fully understood at this stage, but may be dependent on the Ca/surface dosage and related to possible formation of electrostatic bridges. Keller and associates[47] investigated in vitro bone cell attachment and mineralization of modified surfaces by Ca ion implantation and by plasma immersion ion implantation and found no indications of favorable bone cell activity on the ion implantation surfaces. These responses were suggested to be dependent on the Ca/surface dosages used. Krupa and coworkers[48] reported that Ca ion implantation increased corrosion resistance and expressed excellent cellular spreading in a culture of human-derived bone cells. In vitro protein adsorption studies[13,49–51] have suggested that Ca ions of the surface titanium oxides could provide an electrostatic bridge between the titanium surface and adhesive biomolecules in the extracellular bone matrix.

Proteoglycans have been supported as playing a special role in events leading to osseointegration by a number of histochemical, spectroscopic, and biochemical data.[52] Linde and coworkers[53] investigated the mineral induction capacity in vitro of polyanionic proteins of calcified tissues covalently bound to a surface and suggested that phosphoprotein and proteoglycans were responsible for nucleation sites, which initiate mineral formation. Hanawa and associates[9] addressed the increased dielectric constant by Ca^{2+} implantation as a possible reason; this was supported by the findings of Sundgren and colleagues that change in the protein conformation absorbed on the surface was smallest on the material surface having the highest dielectric constant.[54] Sela and coworkers[55] found that differences in matrix mineralization (and also the number and density of matrix vesicles in peri-implant tissue) were associated with the surface chemistry of the implanted materials.

In general, Ca is believed to activate the α and β subunits of integrin, which in turn bind to Arginne-Glycine-Aspartic-acid (RGD) domain of adhesive proteins (fibronectin, vitronection, osteopontin), thus facilitating osteoblast attachment to the implant surface. This may explain the reason for the current histologic findings of greatly pronounced mineralization on the Ca implant surfaces and closer contact of the newly formed bone cells (osteocytes) observed along the Ca implant surface in comparison with turned control implant surfaces.

In essence, plausible explanations can be suggested for some, but certainly not all, of the currently enhanced bone response to the test Ca implants: *(1)* Ca may facilitate the attachment of cells (osteoblasts) via activation of integrin structures and thereby bind to RGD domain of adhesive proteins (fibronectin, vitronection, osteopontin); *(2)* surface Ca chemistry of Ca implants (Ca ≤ 11% incorporation into TiO_2 matrix) may form an electrostatic bond with polyanionic Ca^{+}-binding proteins such as proteoglycan, osteocalcin, osteopontin, and osteonectin in bone matrix; and *(3)* Ca cations in the Ca implant may provide the binding sites involved in any stages of the following biologic mineralization pathway for a variety of Ca phosphate mineral forms[50,56–59]:

$$Ca + PO_4 + 3H_2O \leftrightarrow CaHPO_4{\cdot}2H_2O + OH^- \quad (1)$$

$$7\ Ca + 5PO_4 + 3H_2O + CaHPO_4\cdot 2H_2O \leftrightarrow Ca_8H(PO_4)_6\cdot\ 5H20 \quad (2)$$

$$Ca + Ca_8H_2(PO_4)_6\cdot 5H_2O \leftrightarrow Ca_{9-x}H_{2x}(PO_4)_6 + nH_2O \quad (3)$$

$$Ca + Ca_9(PO_4)_6 + 2H_2O \leftrightarrow Ca_{10}(PO_4)_6(OH)_2 + 2H^+ \quad (4)$$

Surface Ca ions of the Ca-deposited implant in the present study bind with phosphate ions in the extracellular body fluid (Equation 1). During the physiologic function of the implant, movement of Ca ions on the Ca-deposited implant to the outermost surface layer[60] accelerate Ca phosphate formation on the implant surface (Equations 2 to 4).

The present study has focused on early tissue reactions to titanium implants. Further studies are planned with investigations of tissue reactions to Ca-incorporated implants in comparison to calcium phosphate-coated and surface-enlarged implants.

CONCLUSIONS

Ca-reinforced, oxidized titanium implants by the MAO process significantly enhanced bone responses, as measured with biomechanical tests and histomorphometry. The reinforced osseointegration was not the result of differences in surface roughness, but was rather dependent on the surface chemical properties of the electrochemically calcium-incorporated titanium oxide. The present results implicate potential chemical reactions between surface calcium chemistry and bone tissue. Further investigations are needed for better understanding of chemical bonding ability of calcium-incorporated titanium implants.

ACKNOWLEDGMENTS

This study was supported by grants from the Sylvan Foundation, the Hjalmar Svensson Research Foundation, the Medical Research Council, and the Korean Osseointegration Research Institute Foundation.

REFERENCES

1. Testori T, Wiseman L, Woolfe S, Porter SS. A prospective multicenter clinical study of the Osseotite implant: Four-year interim report. Int J Oral Maxillofac Implants 2001; 16:193–200.
2. Buser D, Nydegger T, Oxland T, et al. Interface shear strength of titanium implants with a sandblasted and acid etched surface: A biomechanical study in the maxilla of miniature pigs. J Biomed Mater Res 1999;45:75–83.
3. Palmer RM, Palmer PJ, Smith BJ. A 5-year prospective study of Astra single tooth implants. Clin Oral Implants Res 2000;11:179–182.
4. Albrektsson T, Johansson C, Lundgren AK, Sul YT, Gottlow J. Experimental studies on oxidized implants. A histomorphometrical and biomechanical analysis. Appl Osseointegration Res 2000;1:21–24.
5. Wennerberg A. On Surface Roughness and Implant Incorporation [thesis]. Göteborg: Dept of Biomaterials/Handicap Research, University of Göteborg, Sweden, 1996.
6. Wong M, Eulenberger J, Schenk R, Hunziker E. Effect of surface topology on the osseointegration of implant materials in trabecular bone. J Biomed Mater Res 1995;29:1567–1575.
7. Brunette DM, Chehroudi B. The effects of the surface topography of micromachined titanium substrata on cell behavior in vitro and in vivo. J Biomech Eng-T Asme 1999; 121:49–57.
8. Sul YT, Johansson CB, Jeong Y, Roser K, Wennerberg A, Albrektsson T. Oxidized implants and their influence on the bone response. J Mater Sci Mater Med 2001;12:1025–1031.
9. Hanawa T, Kamiura Y, Yamamoto S, et al. Early bone formation around calcium-ion-implanted titanium inserted into rat tibiae. J Biomed Mater Res 1997;36:131–136.
10. Fujibayashi S, Nakamura T, Nishiguchi S, et al. Bioactive titanium: Effect of sodium removal on the bone-bonding ability of bioactive titanium prepared by alkali and heat treatment. J Biomed Mater Res 2001;56:562–570.
11. Howlett CR, Evans MDM, Wildish KL, et al. The effect of ion implantation on cellular adhesion. Clin Mater 1993;14: 57–64.
12. Ellingsen JE, Pinholt EM. Pretreatment of titanium implants with lanthanum ions alters the bone reaction. J Mater Sci Mater Med 1995;6:125–129.
13. Ellingsen JE. A study on the mechanism of protein adsorption to TiO_2. Biomaterials 1991;12:593–596.
14. Shirkhanzadeh M. Nanoporous alkoxy-derived titanium oxide coating: A reactive overlayer for functionalizing titanium surface. J Mater Sci Mater Med 1998;9:355–362.
15. Wen HB, de Wijn JR, Cui FZ, de Groot K. Preparation of calcium phosphate coatings on titanium implant materials by simple chemistry. J Biomed Mater Res 1998;41:227–236.
16. Lo WJ, Grant DM, Ball MD, et al. Physical, chemical, and biological characterization of pulsed laser deposited and plasma sputtered hydroxyapatite thin films on titanium alloy. J Biomed Mater Res 2000;50:536–545.
17. Rawlings RD. Bioactive glasses and glass ceramics. Clin Mater 1993;14:155–179.
18. Haddow DB, James PF, Van Noort R. Sol-gel derived calcium phosphate coatings for biomedical applications. J Sol-Gel Sci Techn 1998;13:261–265.
19. Ishizawa H, Ogino M. Thin hydroxyapatite layers formed on porous titanium using electrochemical and hydrothermal reaction. J Mater Sci Mater Med 1996;31:6279–6284.
20. Sul YT, Johansson CB, Jeong Y, Albrektsson T. The electrochemical oxide growth behaviour on titanium in acid and alkaline electrolytes. Med Eng Phys 2001;23:329–346.
21. Ciliberto E, Spoto G. Fluorapatite coatings by metal organic chemical vapor deposition. Chem Commun 1997;16: 1483–1484.
22. Bacakova L, Stary V, Kofronova O, Lisa V. Polishing and coating carbon fiber reinforced carbon composites with a carbon-titanium layer enhances adhesion and growth of osteoblast-like MG63 cells and vascular smooth muscle cells in vitro. J Biomed Mater Res 2001;54:567–578.
23. Hanawa T. In vivo metallic biomaterials and surface modification. Mater Sci Eng A Struct 1999;267:260–266.
24. Pham MT, Maitz MF, Matz W, Reuther H, Richter E, Steiner G. Promoted hydroxyapatite nucleation on titanium ion-implanted with sodium. Thin Solid Films 2000;379:50–56.
25. Thorwarth G, Mandl S, Rauschenbach B. Plasma immersion ion implantation using titanium and oxygen ions. Surf Coat Tech 2000;128-129:116–120.

26. Noack N, Willer J, Hoffmann J. Long-term results after placement of dental implants: Longitudinal study of 1,964 implants over 16 years. Int J Oral Maxillofac Implants 1999; 14:748–755.
27. Akagawa Y, Ichikawa Y, Nikai H, Tsuru H. Interface histology of unloaded and early loaded partially-stabilized zirconia endosseous implant in initial bone healing. J Prosthet Dent 1993;69:599–604.
28. Fartash B. Single Crystal Sapphire Dental Implants: Experimental and Clinical Studies [thesis]. Stockholm: Karolinska Institute, 1996.
29. LeGeros RZ. Biodegradation and bioresorption of calcium phosphate ceramics. Clin Mater 1993;14:65–88.
30. Oonishi H, Oomamiuda K. Degradation/resorption in bioactive ceramics in orthopaedics. In: Black J, Hastings G (eds). Handbook of Biomaterial Properties. London: Chapman & Hall, 1998:355–363.
31. Hamadouche M, Meunier A, Greenspan DC, et al. Long-term in vivo bioactivity and degradability of bulk sol-gel bioactive glasses. J Biomed Mater Res 2001;54;560–566.
32. Albrektsson T. Hydroxyapatite-coated implants: A case against their use. J Oral Maxillfac Surg 1998;56:1312–1326.
33. Spector M, Villars PA, Hsu HP, et al. Strength of attachment of bone to hydroxyapatite coated and calcium ion implanted titanium in a canine model. In: Smith DC (ed). Proceedings of the 20th Annual Meeting of the Society for Biomaterials, Boston,1994:330.
34. Ichikawa T, Hanawa T, Ukai H, Murakami K. Three-dimensional bone response to commercially pure titanium, hydroxyapatite, and calcium-ion-mixing titanium in rabbits. Int J Oral Maxillofac Implants 2000;15:231–238.
35. Yoshinari M, Oda Y, Ueki H, Yokose S. Immobilization of bisphosphonates on surface modified titanium. Biomaterials 2001;22:709–715.
36. Nayab S, Shinawi L, Jones FH, et al. Bone cell responses to ion-implanted titanium surfaces. Proceedings of European Society for Biomaterials. London, 2001.
37. Sul YT. On the Bone Response to Oxidized Titanium Implants: The Role of Microporous Structure and Chemical Composition of the Surface Oxide in Enhanced Osseointegration [thesis]. Göteborg: Dept of Biomaterials/Handicap Research, University of Göteborg, Sweden, 2002.
38. Sul YT, Johansson CB, Kang YM, Jeon DG, Albrektsson T. Bone reactions to oxidized titanium implants with electrochemically anion S and P incorporation. Clin Implant Dent Rel Res 2002;4:478–487.
39. Sul YT, Johansson CB, Petronis S, et al. Characteristics of the surface oxides on turned and electrochemically oxidized pure titanium implants up to dielectric breakdown: The oxide thickness, micropore configurations, surface roughness, crystal structure and chemical composition. Biomaterials 2002;23:491–501.
40. Johansson CB. On Tissue Reactions to Metal Implants [thesis]. Göteborg: Dept of Biomaterials/Handicap Research, University of Göteborg, Sweden, 1991.
41. Donath K. Preparation of histologic sections by cutting-grinding technique for hard tissue and other materials not suitable to be sectioned by routine methods. Norderstedt: EXAKT-Kulzer Publications, 1993:1–16.
42. Sul YT, Johansson CB, Jeong Y, Wennerberg A, Albrektsson T. Resonance frequency and removal torque analysis of implants with turned and anodized surface oxides. Clin Oral Implants Res 2002;13:252–259.
43. Sul YT, Johansson CB, Roser K, Albrektsson T. Qualitative and quantitative observations of bone tissue reactions to anodised implants. A histologic, enzyme histochemical and histomorphometric analysis. Biomaterials 2002;23:1809–1817.
44. Sennerby L, Friberg B, Linden B, Jemt T, Meredith N. A comparison of implant stability in mandibular and maxillary bone using RFA. In: European Commission Demonstration Project, Resonance frequency analysis symposium, Göteborg, Sweden, 2000.
45. Takamura R, Yamamoto S, Fujita R, et al. The bone response of titanium implant with calcium ion implantation [abstract]. J Dent Res 1997;76:1177.
46. Howlett CR. Early bone formation around calcium-ion-implanted titanium inserted into rat tibia [abstract]. J Biomed Mater Res 1999;44:352.
47. Keller JC, Marshall GW, Brown I. Effects of Ca ion-implantation on bone cell responses [abstract]. J Dent Res 1994;73:400.
48. Krupa D, Baszkiewicz J, Kozubowski JA, et al. Effect of calcium-ion implantation on the corrosion resistance and biocompatibility of titanium. Biomaterials 2001;22:2139–2151.
49. Parsegian VA. Molecular forces governing tight contact between cellular surfaces and substrates. J Prosthet Dent 1983;49:838–842.
50. Wuthier RE. Calcification of vertebrate hard tissues: In: Sigel H (ed). Metal Ions in Biological Systems, vol 17. New York: Marcel Dekker, 1984:412–472.
51. Collis JJ, Embery G. Adsorption of glycosaminoglycans to commercially pure titanium. Biomaterials 1992;13:548–552.
52. Klinger MM, Rahemtulla F, Prince CW, Lucas LC, Lemons JE. Proteoglycans at the bone-implant interface. Crit Rev Oral Biol Med 1998;9:449–463.
53. Linde A, Lussi A, Crenshaw MA. Mineral induction by immobilized polyanionic proteins. Calcif Tissue Int 1989;44: 286–295.
54. Sundgren JE, Bodo P, Ivarsson B, Lundstrom I. Adsorption of fibrinogen on titanium and gold surfaces studies by ESCA and ellipisometry. J Colloid Interface Sci 1986;113:530–543.
55. Sela J, Gross UM, Kohavi D, et al. Primary mineralization at the surfaces of implants. Crit Rev Oral Biol Med 2000; 11:423–436.
56. Narasaraju TSB, Phebe DE. Some physico-chemical aspects of hydroxylapatite. J Mater Sci Mater Med 1996;31:1–21.
57. Martin RI, Brown PW. Aqueous formation of hydroxyapatite. J Biomed Mater Res 1997;35:299–308.
58. Pham MT, Matz W, Reuther H, Richter E, Steiner G, Oswald S. Ion beam sensitizing of titanium surfaces to hydroxyapatite formation. Surf Coat Tech 2000;128:313–319.
59. Nancollas GH, Wu WJ. Biomineralization mechanisms: A kinetics and interfacial energy approach. J Cryst Growth 2000;211:137–142.
60. Hanawa T, Asami K, Asaoka K. AES studies on the dissolution of surface oxide from calcium-ion-implanted titanium in nitric acid and buffer solutions. Corrosion Sci 1996;38: 2061–2067.